Effect of strain and electric field on the electronic soft matter in manganite thin films

Tara Dhakal, Jacob Tosado, and Amlan Biswas
Department of Physics, University of Florida, Gainesville, Florida 32611, USA
(Received 24 July 2006; revised manuscript received 24 January 2007; published 21 March 2007)

We have studied the effect of substrate-induced strain on the properties of thin films of the hole-doped manganite $(La_{1-y}Pr_y)_{0.67}Ca_{0.33}MnO_3$ (y=0.4, 0.5, and 0.6) grown on $NdGaO_3$ (NGO) substrates, in order to distinguish between the roles played by long-range strain interactions and quenched atomic disorder in forming the micrometer-scale phase separated state. We show that a fluid phase separated (FPS) state is formed at intermediate temperatures similar to the strain-liquid state in bulk compounds, which can be converted to a metallic state by applying an external electric field. In contrast to bulk compounds, at low temperatures a strain stabilized ferromagnetic metallic (FMM) state is formed in the y=0.4 and 0.5 samples. However, in the y=0.6 sample a static phase separated (SPS) state is formed similar to the strain-glass phase in bulk compounds. Our results suggest that the substrate-induced strain is a function of temperature. Hence, we show that the temperature induced variation of the long-range strain interactions plays a dominant role in determining the properties of thin films of phase-separated manganites.

DOI: 10.1103/PhysRevB.75.092404 PACS number(s): 75.47.Lx, 73.50.Fq, 75.47.Gk, 75.70.−i

Multiphase coexistence in hole-doped manganites is a result of the competition between phases of different electronic, magnetic and structural orders, which leads to properties such as colossal negative magnetoresistance (CMR).[1,2] At low temperatures the two competing phases are the ferromagnetic metallic (FMM) and charge-ordered insulating (COI) phases. In manganites with greater average A-site cation radii ($\langle r_A \rangle$) and consequently a larger effective one-electron bandwidth (W), the pseudocubic FMM phase is favored at low temperatures.[3] When smaller ions such as Pr are substituted at the A-site, the pseudotetragonal (distorted) COI phase then has a comparable free energy to the FMM phase, resulting in micrometer scale phase separation.[4] It was shown that in the presence of quenched disorder introduced by the ions of different radii, the similarity of the free energies leads to coexistence of the two competing phases.[2] However, the observation of martensitic strain accommodation in manganites[5] and fluidlike growth of the FMM phase observed in magnetic force microscopy (MFM) images of phase separated manganites[6] suggest that the phases are not pinned, which can be explained by an alternative model which shows that phase separation occurs due to the different crystal structures of the FMM and COI phases and the resultant long range strain interactions.[1] In fact, due to this behavior the phase separated state in manganites has been described as an "electronic soft matter" state.[2,7] To understand the underlying mechanism for micrometer scale phase separation in manganites and propose possible techinical applications, it is essential to distinguish between the roles played by quenched disorder and long range strain interactions.

If long range strain interactions are the principal cause of phase coexistence then it should be possible to control the elastic energy landscape with substrate induced strain. Strain-induced phase separation has been clearly observed in thin films of $La_{0.7}Sr_{0.3}MnO_3$ grown using laser molecular beam epitaxy[8] and substrate strain is known to affect the nature of structural transitions in ferroelectrics.[9] On the other hand, the effect of quenched disorder can be estimated from the effect of isovalent substitution of La-ions by the smaller Pr-ions. In this paper we report our results on the effect of substrate induced strain and isovalent substitution in thin films of the manganite $(La_{1-y}Pr_y)_{0.67}Ca_{0.33}MnO_3$ (LPCMO), and compare our results to bulk LPCMO. The T-H phase diagram of bulk LPCMO clearly shows two distinct types of phase separation (PS), a strain-liquid (dynamic PS) and a strain-glass (frozen PS) regions.[10] We show that in thin films of LPCMO, a fluid phase separated (FPS) state is formed at intermediate temperatures similar to the strain-liquid state in bulk materials. However, a strain stabilized FMM phase is formed at low temperatures leading to a sharper and larger drop in resistivity compared to bulk samples. The strain stabilized FMM phase transforms to a static phase separated (SPS) state (analogous to the strain-glass state in bulk LPCMO) when the Pr content is increased. The FPS and SPS states were named based on the fluidlike and static behavior of the FMM regions in the temperature range of the FPS and SPS states, respectively, as observed in MFM images of LPCMO.[6] Corresponding to our nomenclature of the phase separated states we show that an external electric field transforms the FPS state to a metallic state whereas there is negligible electric field effect once the sample reaches the SPS state.

We have grown thin films of $(La_{1-y}Pr_y)_{0.67}Ca_{0.33}MnO_3$ (LPCMO) (y=0.4, 0.5, and 0.6) using pulsed laser deposition (PLD). The films were grown in an oxygen atmosphere of 420 mTorr on $NdGaO_3$ (NGO) (110) and $SrTiO_3$ (STO) (100) substrates kept at 820 °C. All the films described in this letter are 30 nm thick and were grown at a rate of about 0.05 nm/s. These growth conditions were optimized to obtain an insulator-to-metal transition temperature while cooling T_{IM} (cooling) close to that observed in bulk compounds of similar composition and the minimum transition width at T_{IM} (cooling). Such an optimization is crucial for mapping the phase diagram of LPCMO, since the properties of thin films of this compound vary markedly depending on the growth conditions. Standard $\theta-2\theta$ x-ray diffraction data show that the films are epitaxial and of a single chemical

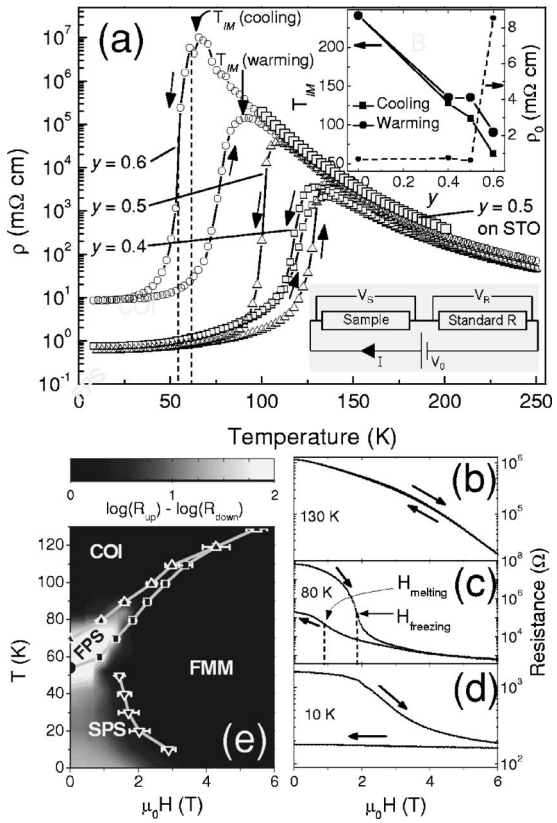

FIG. 1. (a) Resistivity vs temperature curves for thin films of $(La_{1-y}Pr_y)_{0.67}Ca_{0.33}MnO_3$ (y=0.4, 05, and 0.6) on NGO substrates. The open black squares show the resistivity behavior of an LPCMO (y=0.5) film on STO. Cooling and warming directions are indicated by arrows. The dotted lines mark the range of temperatures for the *I-V* curves shown in Fig. 2. The upper inset shows the variation of the transition temperatures and low temperature resistivity (ρ_0) with y. The lower inset shows the setup for measuring the two probe resistance using a constant voltage source. (b), (c), and (d) R vs H curves for the y=0.6 sample in the cooling cycle. (e) The *T-H* phase diagram for the y=0.6 thin film in the cooling cycle.

phase. Since the resistance of the films can be as high as 1 GΩ, the resistivity ρ, of the films was measured with a two-probe method using a constant voltage source, as shown in the lower inset of Fig. 1(a), with V_0 set at 5 V.[11] For the ρ vs T curves, the temperature was varied at a rate of 2 K/min.

The ρ vs T data for three LPCMO films grown on NGO (y=0.4, 0.5, and 0.6) and one LPCMO film grown on STO (y=0.5) are shown in Fig. 1(a). An expected reduction of T_{IM} (cooling) is observed with increasing Pr concentration due to the reduction of $\langle r_A \rangle$. The width of the hysteresis between warming and cooling cycles of temperature drops sharply when y is reduced from 0.5 to 0.4 [Fig. 1(a), top inset]. A remarkable feature of the resistivity is that, unlike in bulk LPCMO,[4] the residual resistivity ρ_0 (measured at 10 K) does not change from y=0 ($La_{0.67}Ca_{0.33}MnO_3$, LCMO) to y=0.5 and then rises sharply for y=0.6 [Fig. 1(a), top inset]. We mapped the *T-H* phase diagram of the y=0.6 sample by measuring resistance R vs H curves at different temperatures for the cooling cycle [Figs. 1(b)–1(d)]. Since the effect of H is irreversible, the sample was reset after every field sweep by heating it to 150 K and then cooling it to the set temperature. The data points were obtained by locating the magnetic field corresponding to the steepest change in R at a given temperature, i.e., where dR/dH is maximum [Fig. 1(c)]. The squares and triangles represent the melting and freezing fields, respectively [Fig. 1(e)]. The melting field line is extended to zero field by including the T_{IM} (cooling) at zero field from Fig. 1(a). The inverted triangles represent the melting field at low temperature ($T \leqslant 50$ K). Since the transition widths can be large in thin films [Fig. 1(d)], as shown by the error bars in Fig. 1(e), we have used a more direct method of constructing the *T-H* phase diagram. We plotted the difference in $\log(R)$ between up sweep and down sweep of H, $\log(R_{up}) - \log(R_{down})$, in the *T-H* plane as a 2D color plot [Fig. 1(e)]. The two methods of plotting the phase diagram give similar results except that the SPS region can be clearly distinguished only with the second method. Four distinct regions can be clearly identified in this phase diagram. Two pure phases namely the COI state and the FMM state and two mixed phase states, namely, the fluid phase separated (FPS) state and the static phase separated (SPS). As mentioned earlier, the nomenclature of the mixed phase states is based on the electric field effect (explained in the following sections) and the previously reported MFM images of LPCMO thin films.[6]

To elucidate the nature of phase coexistence in our thin films of LPCMO we have to understand the combined effect of substrate induced strain and Pr substitution. NGO (110) has an orthorhombic structure with two in-plane distances of 3.853 and 3.861 Å at room temperature, which stabilizes the pseudocubic structure with negligible strain when manganites such as LCMO are grown on NGO.[12] Hence the substrate tends to stabilize the pseudocubic FMM phase at low temperatures in LPCMO samples grown on NGO (110) substrates. Conversely, Pr has a smaller cation radius than La and hence, substitution of La ions by Pr ions favors a distorted crystal structure.[13] The distortion produced by Pr-substitution reduces the T_{IM} (cooling) in our LPCMO thin films similar to bulk LPCMO.[4] On the other hand, strain induced by the NGO substrate removes the resistivity anomaly at the charge-ordering temperature (T_{CO}) seen in bulk LPCMO,[4] which is an effect of the suppression of the bulk structural transition near T_{CO}.[14] Therefore, although the films are under negligible substrate strain at room temperature, the structural phase separation of the bulk material as the temperature is lowered[4] results in a strain build up in the thin film. A similar effect has been shown for ferroelectric thin films where the strain in the film is released by the formation of domains with different structures aided by the defects in the film.[15] A similar structural separation in manganites would lead to phase separation into FMM and COI regions and the observed reduction of T_{IM} (cooling). Furthermore, the thermal contraction of the substrate modifies the strain landscape leading to the fluid nature of the phases as has been observed in MFM images of LPCMO thin films.[6] A detailed temperature dependent structural study of the thin films is required to verify the above hypothesis. However, it is clear from Figs. 1(a) and 1(e) that in spite of substrate induced strain, the phase diagram of the LPCMO (y=0.6) sample is similar to that of bulk LPCMO.[10]

In contrast to the $y=0.6$ sample, ρ_0 for the $y=0.4$ and 0.5 samples drops to a value consistent with the pure FMM phase of the $y=0$ sample [Fig. 1(a), upper inset]. Magnetization measurements also show that the $y=0.5$ sample has a saturation magnetization (M_{sat}) consistent with a pure FMM phase.[16] Hence, these two samples have a pure FMM phase at low temperatures in contrast to the strain-glass phase observed in bulk LPCMO,[10] because the NGO substrate favors the pseudocubic FMM phase at low temperatures. When the Pr concentration is increased to $y=0.6$, ρ_0 increases by about an order of magnitude to 8.7 mΩ cm. The value of M_{sat} for this sample is consistent with 50% of the material being in the FMM phase at low temperatures. As shown in Fig. 1(e), a phase similar to the strain glass phase in bulk LPCMO (the SPS state) appears in the phase diagram of thin film LPCMO only when the Pr concentration is increased to $y=0.6$. It was suggested in Ref. 10 that the strain-liquid to strain-glass transition is due to the interaction of the long-range strain with the quenched atomic disorder. The observation of the FPS state and the absence of the SPS state in the $y=0.5$ sample show that under substrate induced strain, long-range strain is the driving force behind micrometer scale phase separation in manganites. Figure 1(a) also shows the resistivity of a $y=0.5$ film on an STO (100) substrate (STO has a cubic structure with a lattice constant of 3.905 Å which translates to a biaxial tensile strain of 1.2% for a thin film of a manganite such as LCMO grown on STO). The film was insulating down to the lowest temperature of 5 K (data not shown down to 5 K due to high resistance values) which suggests a large strain effect. However, atomic force microscope images revealed different growth modes for the films on NGO and STO which makes it impossible to quantify the change in the strain on these two different substrates since it is known that different growth modes lead to different local strain distributions.[12]

To realize potential applications, an accessible handle is needed to manipulate the phase separation in these thin films and one candidate is an external electric field. Previous measurements of the electric field effect showed a large drop in the resistivity of charge-ordered manganites on the application of an electric field.[17] Electric field effects have also been observed in thin films of LPCMO.[18] Large electric current effects have been observed in LPCMO crystals due to Joule heating of the metallic regions.[19] In our samples, the voltage was applied to the LPCMO thin films using two indium contacts 0.75 mm apart. The circuit for measuring the I-V curves is the same as the one used for measuring resistivity.[11] Figure 2(a) shows the I-V curves for the $y=0.6$ sample for the cooling run. At a threshold voltage V_{th}, the current across the film rises abruptly. This electric field effect is irreversible as shown for the 59 K curve in Fig. 2(a). The sample stays in the low resistance state even when the electric field is removed. To recover the high resistance state we heat the film to a temperature above the resistivity hysteresis region and then cool it down to the next desired temperature. We have plotted the quantity $\log(dI/dV)$ calculated from these I-V curves as a function of temperature and voltage to construct a T-V phase diagram as shown in Fig. 2(b). The observed electric field effect is not a heating effect as reported by Tokunaga *et al.*[19] since heating should increase the resistance

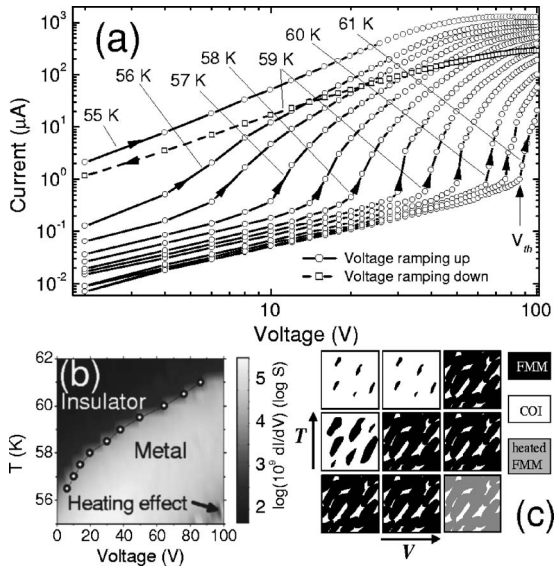

FIG. 2. (a) I-V curves of the $(La_{1-y}Pr_y)_{0.67}Ca_{0.33}MnO_3$ ($y=0.6$) thin film in the cooling cycle with the voltage being ramped up. The dashed curve is the I-V curve at 59 K with the voltage being ramped down. (b) The T-V phase diagram for the $y=0.6$ thin film in the cooling cycle. (c) Schematic representation of the phase coexistence in the T-V plane.

in the temperature range shown in Fig. 2(a). We also observed a similar electric field effect while cooling the $y=0.5$ sample.

Using an extended double exchange Hamiltonian, Gu *et al.* showed that the application of an electric field favors the FMM phase over the COI phase.[20] The authors also showed that V_{th} decreases as the number of high resistance elements is decreased from a 100 to 50 % of the sample, which qualitatively agrees with the observed variation of V_{th} as a function of temperature shown in Fig. 2(b) (decreasing temperature is analogous to decreasing number of high resistances). A schematic picture of the phase coexistence in LPCMO for the cooling cycle in the T-V plane is shown in Fig. 2(c). As the size of the metallic regions (shown in black) increases, the local electric field across the smaller insulating regions (shown in white) is enhanced, which leads to the predicted and observed decrease in V_{th} with decreasing temperature. Above V_{th}, percolation of the metallic regions in the film results in the sharp rise in the conductivity of the film. Further rise in the voltage across the film increases the current flowing through the metallic regions resulting in local heating and a decrease in conductivity similar to the results of Ref. 19 as seen in Fig. 2(b) [gray regions in Fig. 2(c)]. When the sample is cooled down to the SPS state, the metallic regions form a percolating path and increasing the voltage across the sample only results in a larger current and Joule heating. In contrast to the cooling run, no sharp increase in current was observed during the warming run as shown in Fig. 3, which suggests that there is no enhancement of the local electric field. This is due to the static FMM regions in the warming run.[6] The I-V behavior during cooling for a similar resistance value is shown for comparison. Therefore, once the sample is cooled to the SPS region, the FMM and

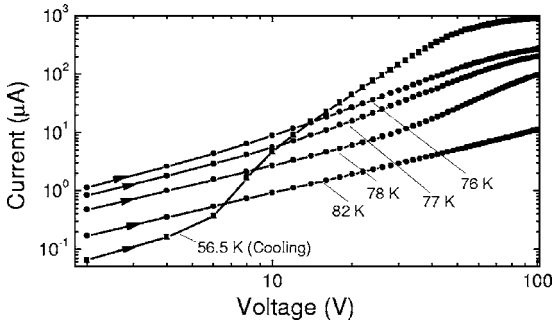

FIG. 3. *I-V* curves of the $(La_{1-y}Pr_y)_{0.67}Ca_{0.33}MnO_3$ ($y=0.6$) thin film in the warming cycle with the voltage being ramped up. The *I-V* curve at 56.5 K for the cooling cycle is shown for comparison.

COI phases are locked in space. Since the FMM regions percolate through the sample, application of a voltage leads to Joule heating of the FMM regions. On further warming the FMM regions homogeneously transform to a high temperature insulating phase with no local enhancement of the electric field.

In conclusion, substrate induced strain modifies the mechanism of micrometer-scale phase separation in manganites. At intermediate temperatures [$T \sim T_{IM}$ (cooling)], long-range strain interactions lead to a fluid phase separated state analogous to the strain-liquid phase in bulk LPCMO.[10] However, below a critical Pr concentration ($y \leqslant 0.5$) the FPS state transforms to a strain stabilized FMM phase at low temperatures, unlike the strain-liquid to strain-glass transition in bulk LPCMO.[10] A static phase separated state analogous to the strain-glass phase in bulk LPCMO is observed at low temperatures only when the Pr concentration (and hence the quenched atomic disorder) is increased above a critical value ($y \geqslant 0.6$). An external electric field provides an effective means to modify the phase separation in manganites since it lowers the resistance of the FPS state by two orders of magnitude due to a local electric field enhancement. However, an electric field has negligible effect on the SPS state. Further experiments using low temperature MFM are needed to find the microscopic mechanism of the electric field effect.

[1] K. H. Ahn, T. Lookman, and A. R. Bishop, Nature (London) **428**, 401 (2004).
[2] E. Dagotto, Science **309**, 257 (2005).
[3] H. Y. Hwang, S.-W. Cheong, P. G. Radaelli, M. Marezio, and B. Batlogg, Phys. Rev. Lett. **75**, 914 (1995).
[4] M. Uehara, S. Mori, C. H. Chen, and S.-W. Cheong, Nature (London) **399**, 560 (1999).
[5] V. Podzorov, B. G. Kim, V. Kiryukhin, M. E. Gershenson, and S-W. Cheong, Phys. Rev. B **64**, 140406(R) (2001).
[6] Liuwan Zhang, Casey Israel, Amlan Biswas, R. L. Greene, and Alex de Lozanne, Science **298**, 805 (2002).
[7] G. C. Milward, M. J. Calderón, and P. B. Littlewood, Nature (London) **433**, 607 (2005).
[8] C. Aruta, G. Ghiringhelli, A. Tebano, N. G. Boggio, N. B. Brookes, P. G. Medaglia, and G. Balestrino, Phys. Rev. B **73**, 235121 (2006).
[9] Y. L. Li, S. Y. Hu, Z. K. Liu, and L. Q. Chen, Acta Mater. **50**, 395 (2002).
[10] P. A. Sharma, Sung Baek Kim, T. Y. Koo, S. Guha, and S-W. Cheong, Phys. Rev. B **71**, 224416 (2005); L. Ghivelder and F. Parisi, *ibid.* **71**, 184425 (2005).
[11] We measured the voltage V_R across the standard resistor R. The current in the circuit then was V_R/R and the voltage across the sample $V_S=V_0-V_R$. Hence, the sample resistance $R_S=(V_0-V_R)\times R/V_R$. As a check, the low temperature resistivity was also measured using a standard four-probe method. The *I-V* curves were measured by varying V_0.
[12] Amlan Biswas, M. Rajeswari, R. C. Srivastava, Y. H. Li, T. Venkatesan, R. L. Greene, and A. J. Millis, Phys. Rev. B **61**, 9665 (2000); Amlan Biswas, M. Rajeswari, R. C. Srivastava, T. Venkatesan, R. L. Greene, Q. Lu, A. L. de Lozanne, and A. J. Millis, *ibid.* **63**, 184424 (2001).
[13] D. E. Cox, P. G. Radaelli, M. Marezio, and S-W. Cheong, Phys. Rev. B **57**, 3305 (1998).
[14] W. Prellier, Amlan Biswas, M. Rajeswari, T. Venkatesan, and R. L. Greene, Appl. Phys. Lett. **75**, 397 (1999).
[15] W. Pompe, X. Gong, Z. Suo, and J. S. Speck, J. Appl. Phys. **74**, 6012 (1993).
[16] M_{sat} is estimated by measuring the *M-H* loops for the thin films and then subtracting the paramagnetic background due to the NGO substrate.
[17] A. Asamitsu, Y. Tomioka, H. Kuwahara, and Y. Tokura, Nature (London) **388**, 50 (1997).
[18] N. K. Pandey, R. P. S. M. Lobo, and R. C. Budhani, Phys. Rev. B **67**, 054413 (2003).
[19] M. Tokunaga, Y. Tokunaga, and T. Tamegai, Phys. Rev. Lett. **93**, 037203 (2004); M. Tokunaga, H. Song, Y. Tokunaga, and T. Tamegai, *ibid.* **94**, 157203 (2005).
[20] R. Y. Gu, Z. D. Wang, and C. S. Ting, Phys. Rev. B **67**, 153101 (2003).